Self-mixing type of phase-locked laser diode interferometer

Takamasa Suzuki, MEMBER SPIE
Shigeyuki Hirabayashi
Osami Sasaki, MEMBER SPIE
Takeo Maruyama
Niigata University
Faculty of Engineering
8050 Ikarashi 2
Niigata 950-2181
Japan
E-mail: takamasa@eng.niigata-u.ac.jp

Abstract. A new type of phase-locked laser diode interferometer that uses self-mixing interference in the optical system is described. The self-mixing interference (SMI) signal is obtained easily by optical feedback, i.e., feeding back the laser beam from the object to the laser diode (LD). The SMI signal can be detected by a photodiode in the package of the LD. Therefore, a beamsplitter, reference mirror, and external photodetector are not required, and an interference signal is obtained using a simple optical system. Although the mechanism of SMI is completely different from that of conventional interference, it is shown that the response of the SMI signal to phase changes is the same as that of conventional interference. We used the phase-locked technique to fix the phase change and demonstrated measurement of absolute distance and displacement. [S0091-3286(99)01503-2]

Subject terms: optical feedback; self-mixing; laser diode; phase lock; range finder; displacement measurement.

Paper 980151 received Apr. 17, 1998; revised manuscript received Aug. 25, 1998, and Oct. 1, 1998; accepted for publication Oct. 5, 1998.

1 Introduction

The self-mixing effect, or external optical feedback, with a laser diode (LD) has been investigated theoretically[1-4] with respect to spectral change. It has also been applied to linewidth reduction[5] and broadening.[6] Self-mixing can be easily realized by feeding back the laser beam from the external reflector to the LD. The LD incorporates a photodiode (PD) for monitoring optical power. This PD can be used for detecting the self-mixing signal. With a simply constructed optical system, the self-mixing effect has been applied to many kinds of optical sensors[7,8] and Doppler velocimeters.[9-11]

The signal obtained by the self-mixing effect is a kind of interference signal and is called the self-mixing interference (SMI) signal.[12] Since a beamsplitter, reference mirror, and external photodetector are not required for the self-mixing type of interferometer, the optical system is very simple compared with conventional interferometers. Previously, measurement systems which take the place of interferometers have proposed, including rangefinders,[13-16] displacement sensors,[17] and profilometers.[18,19] The SMI signal, however, is completely different from the signal obtained in a conventional interferometer in that it takes a sawtooth form[10,12-14] when the LD is directly modulated with the injection current or when the phase of the returning laser beam is changed by the displacement of the external reflector.

When the LD is modulated by the triangular modulating current, the number of mode hops[14] or the period of the SMI signal[15] varies with the distance between the LD and the external reflector or the target. In rangefinding, the target range can be measured by detecting the number of mode hops or the period of the SMI signal. However, it is difficult to determine range accurately using mode-hop or SMI-period methods. Although displacement measurement[17] may be realized by detecting the change of intensity or phase of the SMI signal in one period, phase detection is as difficult as in conventional interferometers, and its accuracy depends on the phase-detecting process.

In this paper, we propose the phase-locked type[20-22] of self-mixing interferometer, and we demonstrate measurements of absolute distance and microscopic displacement. The phase-lock technique is useful in eliminating external disturbances and in fixing the phase of the SMI signal at a specific value. Absolute distance is not measured by the period, but by the frequency of the SMI signal under feedback control. Displacement is measured using conventional phase-locked laser diode (PLLD) interferometry. Displacement measurement is not implemented by numerical calculation, but by feedback control in PLLD interferometry. Thus, the measurement can be performed in real time, and special signal processing is not required. Also, the optical system is very simple compared with the conventional PLLD interferometer.

The principles of SMI signal generation are described in the next section. We also explain how to apply the PLLD technique to the self-mixing type of interferometer, and the principles of ranging and displacement measurement are described. The experimental setup is described in Sec. 3, and results and discussions are given in Sec. 4.

2 Principles of SMI Signal Generation

2.1 *SMI Signal*

A schematic of the SMI effect in a LD package is shown in Fig. 1. The SMI is realized by a package consisting of the LD, a lens, and an external mirror as shown in Fig. 1(a). The distance between the LD and the external mirror is D_0.

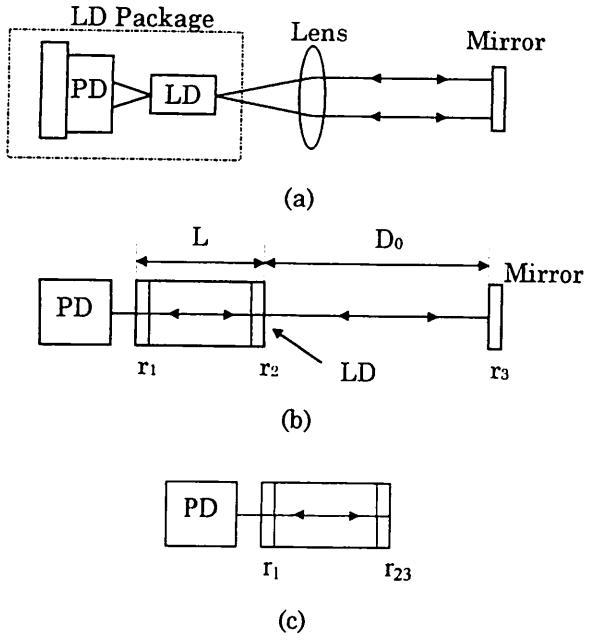

Fig. 1 Schematic of (a) SMI effect in an LD package, (b) external-cavity laser diode, and (c) an equivalent system.

In this case, the PD in the LD package can be used as a photodetector for the SMI signal. The SMI effect is explained by a model of the external-cavity laser diode[8,23-25] shown in Fig. 1(b). The external mirror of amplitude reflectivity r_3 is coupled to the LD, and we assume that reflectivities on the two edges of the LD are r_1 and r_2, respectively. Then the equivalent system is represented by Fig. 1(c), in which an effective reflectivity on the facet of the LD is

$$r_{23}=\frac{r_2-r_3\exp(i\alpha_0)}{1-r_2r_3\exp(i\alpha_0)}, \tag{1}$$

where

$$\alpha_0=\frac{4\pi D_0}{\lambda_0}. \tag{2}$$

In this case, the threshold current I_{th} of the LD shown in Fig. 1(c) is[25]

$$I_{th}=\eta\left[\gamma_i+\frac{1}{2L}\ln\left(\frac{1}{r_1r_{23}}\right)\right]. \tag{3}$$

Here r_{23} is the effective reflectivity, η is a constant determined by the gain medium and its size, γ_i is an internal loss coefficient, and L is the cavity length of the LD. Equation (2) shows that the phase α_0 depends on the distance D_0 and on the wavelength λ_0. Therefore, when D_0 varies with the displacement of the mirror or when λ_0 varies with the LD injection current, the threshold current I_{th} changes according to Eqs. (1)–(3). However, the output power $P_o(t)$ of the LD varies with the injection current $I(t)$, which is larger than I_{th}, and is[26]

$$P_o(t)=\kappa\left[\frac{I(t)}{I_{th}}-1\right], \tag{4}$$

where κ is a constant which can be easily determined experimentally. Consequently, the displacement of the mirror is reflected in a change of the optical output P_o. We can detect this change as an interference signal. Although the mechanism of the optical intensity change is obviously different from that in a conventional interferometer, the optical output P_o can be controlled by adjusting α_0, so that PLLD interferometry is applicable to the SMI system.

2.2 *Measurement of Distance*

For distance measurement the LD is modulated by a triangular current

$$I_m(t)=\pm at, \tag{5}$$

where a is the slope of the current. Noting that the wavelength of the LD varies with the injection current, and using a negative slope for $I_m(t)$, the phase of the SMI signal from Eq. (2) is

$$\alpha(t)=\frac{4\pi D_0}{\lambda_0-\beta at}\approx 2\pi f_c t+\alpha_0, \tag{6}$$

where

$$f_c=\frac{2D_0}{\lambda_0^2}a\beta \tag{7}$$

is a beat frequency that depends on the optical path difference $2D_0$, and β is the modulation efficiency of the LD. The first term varies with time, and the second term is a constant phase that is determined by the wavelength and the optical path difference as shown in Eq. (2). For ranging, we use the first term, that is, if the beat frequency f_c is detected, the distance D_0 is

$$D_0=\frac{\lambda_0^2}{2a\beta}f_c. \tag{8}$$

2.3 *Measurement of Displacement*

For displacement measurement we use the second term in Eq. (6). When the mirror M vibrates with amplitude $d(t)$, the SMI signal phase shown in Eq. (6) is no longer constant. The change is

$$\alpha(t)=\frac{4\pi}{\lambda_0}[D_0+d(t)]. \tag{9}$$

In the PLLD interferometry, we make the deviated phase in Eq. (9) equal the initial phase α_0 by changing the LD wavelength. This compensation is achieved by the electrical feedback control on the LD injection current. Thus, the relationship

$$\frac{4\pi}{\lambda_0+\beta I_c(t)}[D_0+d(t)]=\frac{4\pi}{\lambda_0}D_0 \tag{10}$$

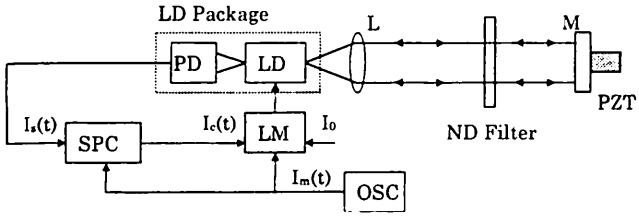

Fig. 2 Experimental setup of the PLLD self-mixing interferometer: LD, laser diode; PD, photodiode in the LD package; LM, LD modulator; OSC, oscillator; SPC, signal processing circuit.

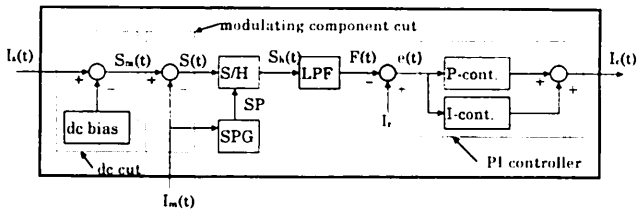

Fig. 3 Block diagram of the SPC: S/H, sample and hold circuit; SPG, sampling pulse generator; LPF, low-pass filter.

is realized automatically, where $I_c(t)$ is the feedback control current.

From Eq. (10) the displacement of the mirror is given by[20]

$$d(t)=\frac{D_0}{\lambda_0}\beta I_c(t). \tag{11}$$

The displacement is proportional to the control current $I_c(t)$. Therefore, we can measure displacement by observing $I_c(t)$.

3 Experimental Setup

The experimental setup is shown in Fig. 2. Experiments were performed with a cw GaAlAs multi-quantum-well (MQW) LD (Hitachi HL7851G). The linearity between wavelength and injection current is good for this type of LD. The optical system consists of the LD, a lens L, a neutral-density (ND) filter, and an object mirror M. The mirror is mounted on a piezoelectric transducer (PZT). The central wavelength λ_0, maximum output power, and modulation efficiency β of the LD are 785 nm, 50 mW, and 2.0×10^{-3} nm/mA, respectively. The distance between the exit face of the LD and the object mirror M is D_0. It can be changed by a micrometer on an x-axis stage. Since mirror M is at a distance from the LD in our setup, it might suffer instabilities from excursions of the feedback beam. This problem, however, is addressed using an optical fiber that is fixed in front of the exit face of the LD. The interference signal detected by the PD in the LD package is processed with a signal-processing circuit (SPC), which generates a control current $I_c(t)$ for the phase lock. The injection current of the LD consists of dc bias current I_0, triangular modulating current $I_m(t)$, and control current $I_c(t)$. These currents are mixed in the laser modulator LM and injected into the LD. The current I_0 determines the central wavelength λ_0. The wavelength of the LD is varied slightly around λ_0 by $I_m(t)$ and $I_c(t)$. The current $I_m(t)$ gives phase modulation to the SMI signal, and the current $I_c(t)$ locks the phase of the SMI signal to the desired value by changing the LD wavelength. The intensity ratio between the feedback light from mirror M and the output light of the LD was 5.6%.

A block diagram of the SPC is shown in Fig. 3. The signal $I_s(t)$ detected by the PD contains not only the SMI signal but also the useless dc and modulating components. These useless signals are removed at the front part of the SPC by differential amplifiers. The remaining signal $S(t)$ is passed to the sample-and-hold circuit S/H and a low-pass filter LPF with a cutoff frequency of 100 Hz. The feedback signal $F(t)$ is also generated. The sampling pulse generator SPG defines the sampling time, which must coincide with the time when $S(t)$ has positive slope, because an $S(t)$ of negative slope means positive feedback and introduces instability in the control system.[22] The signal $F(t)$ is compared with a constant reference signal I_r in the differential amplifier, and the error signal $e(t)$ is fed into the proportional-integral (PI) controller. The proportional gain K_p and the integration time T_I of the PI controller can be easily adjusted.

Figure 4 shows schematically how the feedback signal is generated. The sampling pulse SP is generated in the SPG synchronously with $I_m(t)$. The S/H samples $S(t)$ each period of $I_m(t)$ and holds it through the next sampling point. If the mirror is stationary, $S(t)$ is sampled at the same phase and the held signal $S_h(t)$ is temporally constant. However, if the mirror is displaced, the phase of $S(t)$ changes and $S_h(t)$ becomes step-shaped as shown in Fig. 4(c). The LPF shown in Fig. 3 removes higher-frequency components from the step-shaped $S_h(t)$.

4 Experimental Results

The SMI signal and the conventional interference signal were observed without moving the mirror. The distance D_0 was 30 cm. Results are shown in Fig. 5. The trace in Fig. 5(a) is the triangular modulating current $I_m(t)$. Figure 5(b) and 5(c) show the shapes of the original SMI signal and the extracted SMI signal, respectively. They correspond to the signals $S_m(t)$ and $S(t)$ in Fig. 3, respectively. The dc component is eliminated from $S_m(t)$, but it still contains the

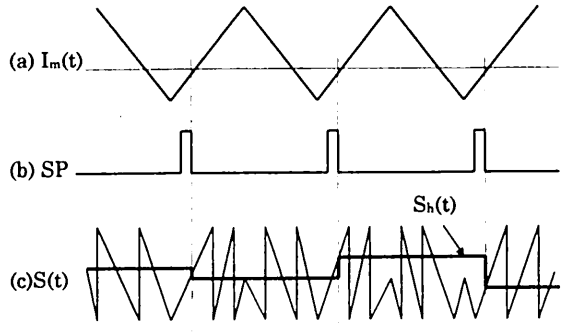

Fig. 4 Generation of the feedback signal for PLLD interferometry: $I_m(t)$, modulating current; SP, sampling pulse; $S(t)$, self-mixing interference signal; $S_h(t)$, generated feedback signal.

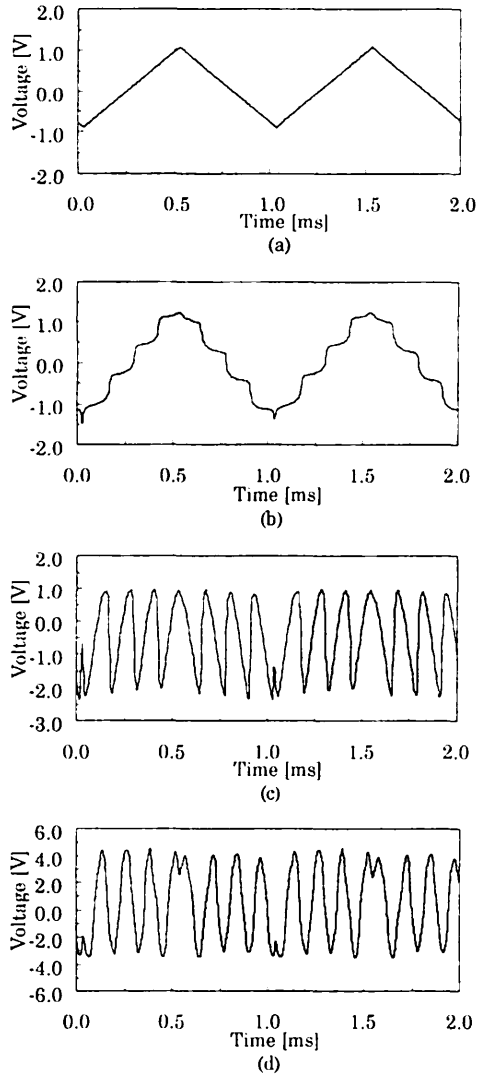

Fig. 5 The SMI signal and the conventional interference signal. The LD is injected with (a) a triangular modulating current $I_m(t)$, and (b) a step-shaped SMI signal is obtained. Upon eliminating the modulating component, a sawtooth SMI signal (c) is obtained, which is different from (d) the conventional interference signal obtained from a two-pass interferometer.

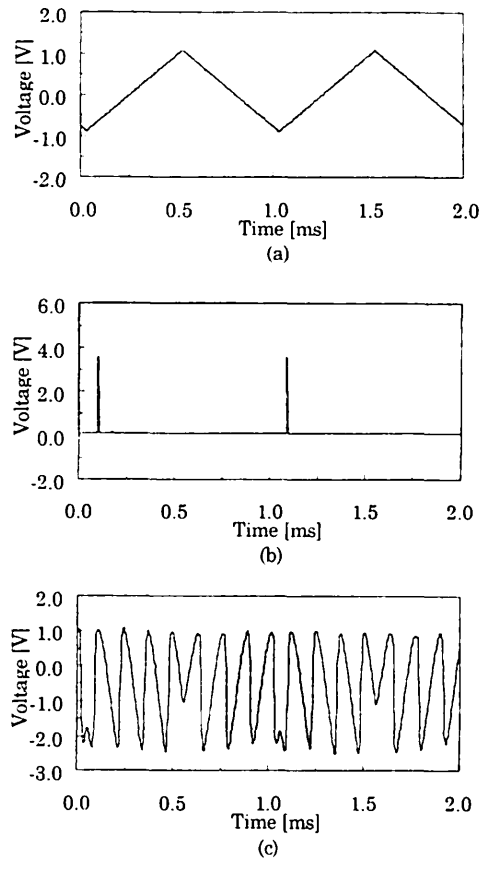

Fig. 6 The SMI signal with feedback control: (a), (b), and (c) are the triangular modulating current, the sampling pulse SP, and the phase-locked SMI signal $S(t)$, respectively. The SP is located between the steepest positive slopes of $S(t)$.

modulated component and shows a triangular form in response to $I_m(t)$. Thus the shape of $S(t)$ is sawtooth-like and is obviously different from the shape of the conventional interference signal shown in Fig. 5(d). The conventional signal is obtained using a Twyman-Green interferometer whose optical path difference is the same as in Fig. 1. Since the phase change introduced by the modulating current is the same in both interference signals, the SMI signal can be used to realize conventional interferometry.

We observed $S(t)$ under phase lock without vibrating the mirror. The proportional gain K_p and the integration time T_I of the PI controller were 0.87 and 2.7 ms, respectively. The results are shown in Fig. 6 and correspond to the diagrams in Fig. 4. Figure 6(a) and 6(b) show $I_m(t)$ and the sampling pulse SP, respectively. The SP is generated in each period of $I_m(t)$. The phase-locked $S(t)$ shown in Fig. 6(c) is distinctive compared with the $S(t)$ shown in Fig. 5(c), which was obtained without feedback control. That is, (1) the external disturbance in $S(t)$ is eliminated by feedback control, and (2) the locations of the steepest positive slopes in $S(t)$ correspond with the locations of the sampling pulses SP, because the feedback loop is most stable where the loop gain is maximum. These features show that the feedback control works well and that phase lock can be achieved in a self-mixing interferometer.

The results of the absolute distance measurement are shown in Figs. 7 and 8. Figure 7 was obtained for a distance D_0 of 30 cm. The frequency and amplitude of the $I_m(t)$ shown in Fig. 7(a) are 1 kHz and 1.02 mA, respectively, and the slope a of $I_m(t)$ is 4.02 mA/ms. The result of a fast Fourier transform (FFT) analysis of the phase-locked SMI signal $S(t)$ shown in Fig. 7(b) is provided in Fig. 7(c). External disturbances in $S(t)$ are largely eliminated by feedback control. The signal $S(t)$ was sampled in a positive region of the modulating current and fed through a window function before the FFT was performed for a sampling frequency of 500 kHz. The maximum spectral intensity is at $f_c = 7.81$ kHz. The absolute distance is obtained as 29.93 cm from Eq. (7). The same kinds of measurements were carried out for several values of D_0, and the results are plotted in Fig. 8. The experimental results, indicated by dots, are fitted by a theoretical line, and the rms deviation from the fitted line was 2.58 mm. Since the frequency reso-

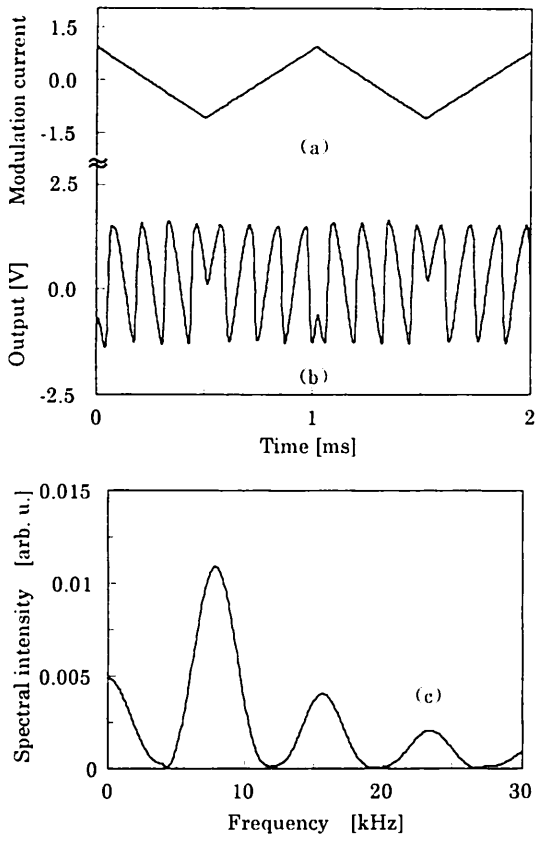

Fig. 7 Experimental example of the spectral intensity of the SMI signal: (a) $I_m(t)$, (b) phase-locked SMI signal, and (c) power spectrum.

lution of the FFT was 61.04 Hz, the accuracy of ranging calculated by Eq. (8) is 2.25 mm, which corresponds to the rms error obtained in the experiment. The maximum measurable range in this method depends on the coherence of the LD. That is, if the SMI signal is detectable, ranging can be performed in principle.

Displacement measurement was demonstrated for rectangular vibration of the mirror. The mirror was vibrated by a PZT at 10 Hz. The frequency and amplitude of $I_m(t)$ were the same as in the previous distance measurement experiments, and measurement results are shown in Fig. 9. Figure 9(a) shows the displacement calculated from the ap-

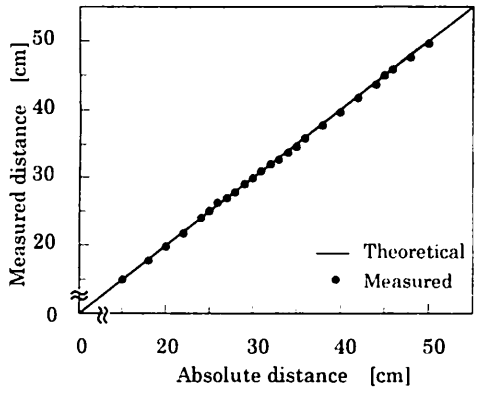

Fig. 8 Results for absolute distance measurements. The mirror was moved from 10 to 50 cm with a micrometer.

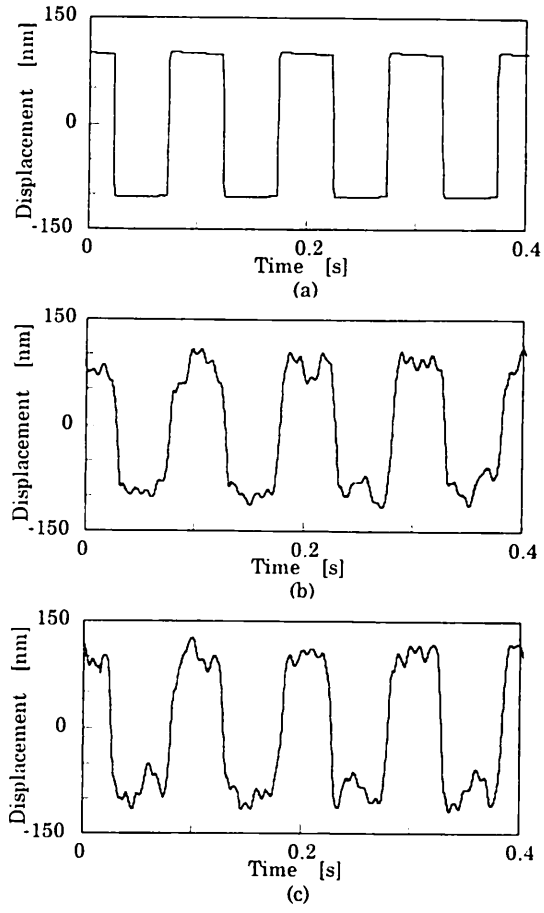

Fig. 9 Results for displacement measurements. The mirror was vibrated with (a) a rectangular wave using the PZT. The results shown in (b) and (c) were obtained for distances D_0 of 20 and 30 cm, respectively.

plied voltage for the PZT. Measurement results obtained when the distance D_0 was 20 and 30 cm are shown in Fig. 9(b) and 9(c), respectively. Although the amplitude of the control current $I_c(t)$ depended on the distance D_0, the results calculated by Eq. (11) gave the same amplitude. These results contain noise of magnitude $\approx \pm 25$ nm. Therefore, displacement measurement error does not exceed 50 nm in our prototype system. It seems that noise generated by the optical feedback in the LD determines the measurement accuracy, because external mechanical disturbance is eliminated by feedback control. Further experiments should examine the reduction of this noise. The maximum measurable range in displacement measurement depends on the stability of the control system. The control system is stable when the sampling pulse is in the region of positive slope of $S(t)$, as mentioned in Sec. 3, which means that the phase of interest or the phase represented in Eq. (10) must be in the region $-\pi/2$ to $+\pi/2$. Thus the measurable range is limited to the region $-\lambda_0/8$ to $+\lambda_0/8$, or -98 to $+98$ nm. The results shown in Fig. 9 are obtained at the maximum measurable range.

5 Conclusion

We have proposed and demonstrated a phase-locked laser diode interferometer that uses the self-mixing effect in the

LD. Since it requires no beamsplitter, no reference mirror, and no external photodetectors, the optical system is very simple. The mechanism of SMI is quite different from that of conventional interferometers, but we have shown that the interference signal can be extracted from the SMI signal and that the behavior of the SMI interference signal is the same as that of the conventional interference signal. Thus the phase of the SMI signal can be compensated by controlling the wavelength of the LD. Absolute distance was measured under phase-lock control, so that the initial phase of the SMI signal was locked and external disturbances were eliminated. Rectangular vibration was measured using conventional PLLD interferometry. Noise induced by optical feedback must be examined and eliminated to improve measurement accuracy.

Acknowledgment

A portion of this work was presented at the SPIE annual meeting[27] in San Diego, California.

References

1. T. Kanda and K. Nawata, "Injection laser characteristics due to reflected optical power," *IEEE J. Quantum Electron.* **QE-15**, 559–565 (1979).
2. R. Lang and K. Kobayashi, "External optical feedback effect on semiconductor injection laser properties," *IEEE J. Quantum Electron.* **QE-16**, 347–355 (1980).
3. N. Schunk and K. Petermann, "Numerical analysis of the feedback regimes for a single-mode semiconductor laser with external feedback," *IEEE J. Quantum Electron.* **24**, 1242–1247 (1988).
4. J. S. Cohen, F. Wittgrefe, M. D. Hoogerland, and J. P. Woerdman, "Optical spectra of a semiconductor laser with incoherent optical feedback," *IEEE J. Quantum Electron.* **26**, 982–990 (1990).
5. G. P. Agrawal, "Line narrowing in a single-mode injection laser due to external optical feedback," *IEEE J. Quantum Electron.* **QE-20**, 468–471 (1984).
6. R. O. Miles, A. Dandridge, A. B. Tevten, H. F. Taylor, and T. G. Giallorenzi, "Feedback-induced line broadening in cw channel-substrate planer laser diodes," *Appl. Phys. Lett.* **37**, 990–992 (1980).
7. Y. Mitsuhashi, T. Morikawa, A. Seko, and J. Shimade, "Self-coupled optical pickup," *Opt. Commun.* **17**, 95–97 (1976).
8. R. O. Miles, A. Dandridge, A. B. Tveten, and T. G. Giallorenzi, "An external cavity diode laser sensor," *J. Lightwave Technol.* **LT-1**, 81–93 (1983).
9. S. Shinohara, A. Mochizuki, H. Yoshida, and M. Sumi, "Laser Doppler velocimeter using the self-mixing effect of a semiconductor laser diode," *Appl. Opt.* **25**, 1417–1419 (1986).
10. E. T. Shimizu, "Direction discrimination in the self-mixing type laser Doppler velocimeter," *Appl. Opt.* **26**, 4541–4544 (1987).
11. H. W. Jentink, F. F. M. de Mul, H. E. Suichies, J. G. Aarnoudse, and J. Greve, "Small laser Doppler velocimeter based on the self-mixing effect in a laser diode," *Appl. Opt.* **27**, 379–385 (1988).
12. W. M. Wang, W. J. O. Boyle, K. T. V. Grattan, and A. W. Palmer, "Self-mixing interference in a diode laser: experimental observations and theoretical analysis," *Appl. Opt.* **32**, 1551–1558 (1993).
13. P. J. de Groot, G. M. Gallatin, and S. H. Macomber, "Ranging and velocimetry signal generation in a backscatter-modulated laser diode," *Appl. Opt.* **27**, 4475–4480 (1986).
14. G. Beheim and K. Fritsch, "Ranging finding using frequency-modulated laser diode," *Appl. Opt.* **25**, 1439–1442 (1986).
15. S. Shinohara, M. Andou, M. Miyata, H. Yoshida, J. Yoshida, K. Nishide, and M. Sumi, "FM-modulation distortion of light output from semiconductor laser modulated with triangular wave current," *Trans. Electron. Info. Commun. Engineers* **E72**, 275–278 (1989).
16. S. Shinohara, H. Yoshida, H. Ikeda, K. Nishide, and M. Sumi, "Compact and high-precision range finder with wide dynamic range and its application," *IEEE Trans Instrum. Meas.* **41**, 40–44 (1992).
17. A. Dandridge, R. O. Milse, and T. G. Giallorenzi, "Diode laser sensor," *Electron. Lett.* **16**, 948–949 (1980).
18. P. J. de Groot, G. Gallatin, G. Gardopee, and R. Dixon, "Laser feedback metrology of optical systems," *Appl. Opt.* **28**, 2462–2464 (1989).
19. P. J. de Groot, "Ranging-dependent optical feedback effect on the multimode spectrum of laser diode," *J. Mod. Opt.* **37**, 1199–1214 (1990).
20. T. Suzuki, O. Sasaki, and T. Maruyama, "Phase-locked laser diode interferometry for surface profile measurement," *Appl. Opt.* **28**, 4407–4410 (1989).
21. T. Suzuki, O. Sasaki, K. Higuchi, and T. Maruyama, "Phase locked laser diode interferometer: high speed feedback control system," *Appl. Opt.* **30**, 3622–3626 (1991).
22. T. Suzuki, T. Muto, O. Sasaki, and T. Maruyama, "Wavelength-multiplexed phase-locked laser diode interferometer using a phase-shifting technique," *Appl. Opt.* **36**, 6196–6201 (1997).
23. A. Olsson and C. T. Tang, "Coherent optical interference effect in external-cavity semiconductor lasers," *IEEE J. Quantum Electron.* **QE-17**, 1320–1323 (1981).
24. T. Yoshino, M. Nara, S. Mnatzakanian, B. S. Lee, and T. C. Strand, "Laser diode feedback interferometer for stabilization and displacement measurements," *Appl. Opt.* **26**, 893–897 (1987).
25. Y. Katagiri and S. Hara, "Increased spatial frequency in interferential undulations of coupled cavity lasers," *Appl. Opt.* **33**, 5564–5570 (1994).
26. P. J. de Groot and G. M. Gallatin, "Backscatter-modulation velocimetry with an external-cavity laser diode," *Opt. Lett.* **14**, 165–167 (1989).
27. T. Suzuki, S. Hirabayashi, O. Sasaki, and T. Maruyama, "Self-mixing type of phase-locked laser diode interferometer," *Proc. SPIE* **3134**, 512–519 (1997).

Takamasa Suzuki received a BE degree in electronic engineering from the Niigata University in 1982, a ME degree in electrical and communication engineering from the Tohoku University in 1984, and a DE degree in engineering from the Tokyo Institute of Technology in 1994. He is an associate professor of electrical and electronic engineering at the Niigata University. His research interests include optical metrology, optical information processing, and phase-conjugate optics.

Shigeyuki Hirabayashi received BE and ME degrees in electrical and electronic engineering from the Niigata University in 1996 and 1998, respectively. He was a graduate student at the Graduate School of the Niigata University when this work was done. He is currently working at Hitachi Co., Ltd., Japan.

Osami Sasaki received BE and ME degrees in electronic engineering from the Niigata University in 1972 and 1974, respectively, and a DE degree in engineering from the Tokyo Institute of Technology in 1981. He is a professor of electrical and electronic engineering at the Niigata University. His research interests include optical metrology, optical information processing, and phase-conjugate optics.

Takeo Maruyama received a BE degree in electrical engineering from the Niigata University in 1965 and a DE degree in engineering from the Nagoya University in 1979. He is a professor of electrical and electronic engineering at the Niigata University. His research interests include the physics of ionized gases and optical metrology.